GEOPHYSICS, VOL. 69, NO. 3 (MAY-JUNE 2004); P. 719–730, 6 FIGS., 1 TABLE.
10.1190/1.1759458

Processing of anisotropic data in the τ-p domain: I—Geometric spreading and moveout corrections

Mirko van der Baan*

ABSTRACT

Stacking of seismic data is conventionally done in the time-offset domain. This has the disadvantage that geometric spreading must be removed before true-amplitude processing can be attempted. This inconvenience arises since wave motion in the time-offset domain is determined by spherical waves. Plane waves in layered media, on the other hand, are not subject to geometric spreading. Hence, processing of both isotropic and anisotropic data in such media benefits from first applying a plane-wave decomposition such as a proper τ-p transform. The resulting τ-p gathers can be flattened and stacked over slowness. Subsequent time differentiation is needed to counter the loss of high frequencies during stacking. This approach has the advantage that the geometric spreading is removed without prior knowledge of the actual (an)isotropic velocity field and without any need to pick traveltimes or moveout velocities. Subsequent moveout corrections naturally require knowledge of the velocity field.

The proposed methodology is exact for 3D data volumes and arbitrary anisotropy in laterally homogeneous media or for 2D acquisition lines over 1D, isotropic media or over 1D, transversely isotropic media with vertical axis of symmetry (VTI). It relies on the same principles as more conventional geometric spreading corrections and time-offset stacking. In many respects, it is even more flexible. For instance, geometric spreading has been correctly removed for all present wave modes and types simultaneously (primary, multiple, pure-mode, and converted waves), and nonhyperbolic moveout resulting from isotropic layering is also taken into account. In addition, head waves may now contribute constructively to the stacked section. Moreover, both multiple elimination and predictive deconvolution are straightforward and known to yield very good results in the τ-p domain. The resulting stacked section can then be used for any poststack processing such as time migration.

INTRODUCTION

Amplitudes of seismic data are affected by a number of factors, including geometric spreading, interface reflection and transmission losses, source and receiver effects (coupling, directivity), attenuation, and multiples. True-amplitude processing requires that at least the principal effects of these factors be understood and accounted for. O'Doherty and Anstey (1971) qualitatively discuss several of these effects and identify geometric spreading as one of the most important factors.

This paper develops a simple methodology to remove geometric spreading of both isotropic and anisotropic media that does not require major changes to the conventional processing stream. For instance, it should still be possible to perform a velocity analysis in the t-x domain if desired. I show that this can be done by first applying a plane-wave decomposition (PWD) on the data. Individual techniques of the proposed τ-p methodology rely on the same approximations as their counterparts in the t-x domain. In some respects they are even less restrictive.

Processing of isotropic data already benefits from initially applying a PWD such as a τ-p transform (Treitel et al., 1982). Plane waves in laterally homogeneous media are not subject to geometric spreading, whereas spherical waves are. Hence, no geometric spreading correction need be applied for pure-mode P–P-waves in an isotropic, laterally homogeneous medium after a PWD (Wang and McCowan 1989; Dunne and Beresford, 1998). As a matter of fact, this is true for all wave modes and types (i.e., pure-mode and converted waves, and primary reflections and multiples). Furthermore, multiple elimination is mathematically easier to implement in the τ-p domain [e.g., Radon-based demultiple techniques; see, e.g., Yilmaz (2001)]. Predictive deconvolution also yields better results after a PWD (Treitel et al., 1982). In addition, it is possible to stack traces in the τ-p domain (Stoffa et al., 1981, 1982). However, whereas traces are stacked over offset after a conventional t-x moveout

Manuscript received by the Editor December 30, 2002; revised manuscript received December 9, 2003.
*University of Leeds, School of Earth Sciences, Leeds LS2 9JT, United Kingdom. E-mail: mvdbaan@earth.leeds.ac.uk.

correction, they are stacked over slowness after a τ-p moveout correction. Subsequent time differentiation is required to compensate for loss of resolution which occurs during the stacking process.

Stacking in the τ-p domain has the further advantage that nonhyperbolic moveout resulting from isotropic layering is accounted for—contrary to the conventional t-x NMO correction which is valid strictly for short-spread data (Taner and Koehler, 1969). Furthermore, reflections do not cross in the τ-p domain, and traveltime triplications (wavefront folding) are unfolded. Both τ-p and t-x NMO corrections can handle the effect of a single dipping layer as long as pure-mode data are sorted in the common midpoint (CMP) domain. However, both break down in the presence of more complicated moderate to strong lateral inhomogeneities. Stacking and processing in the τ-p domain therefore has several potential advantages over the conventional t-x approach.

An additional advantage for anisotropic media is that after a PWD we only need to deal with plane waves, which are described by phase velocities instead of group velocities. Phase velocities are substantially less complex than the corresponding group velocities and directly result from the Christoffel equation. Hence, the mathematical description of wave propagation effects in, for instance, the τ-p domain is substantially simpler than in the t-x domain. This has consequences for anisotropic moveout corrections applied in the τ-p domain.

The application of a PWD therefore has considerable advantages over t-x–based spreading corrections since the latter require knowledge of the anisotropy parameters in the first layer and traveltime picks of major reflectors plus the first and second derivatives of the traveltimes with respect to offset (Ursin, 1990; Zhou and McMechan, 2000). In addition, the latter often lose their accuracy for offset–depth ratios beyond one because of uncertainties in the traveltimes (Zhou and McMechan, 2000). Most importantly, however, correction techniques based on normalized relative spreading in the t-x domain, such as the approaches of Newman (1973), Ursin (1990), and Zhou and McMechan (2000), "cannot simultaneously compensate for both primary and multiple reflections if these are characterized by different rms velocities. As a general rule, primary reflections will incur greater amplitude loss due to divergence than will multiple reflections occurring at similar record times. The effect of this is to increase the significance of multiples, particularly in prospect areas where velocity gradients are steep" (Newman, 1973, p. 484). Similarly, superposed converted waves on an assumingly clean pure-mode section also cause havoc. Neither drawback applies on the PWD methodology proposed here. Finally, all techniques based on the approach of Newman (1973) and Ursin (1990) also assume the presence of lateral homogeneity (i.e., horizontal layering).

In this paper, I demonstrate that geometric spreading corrections are not necessary after a PWD in a laterally homogeneous medium with arbitrary anisotropy and 3D data volumes in general and for 2D data lines in a 1D, isotropic, or transversely isotropic with vertical axis of symmetry (VTI) medium in particular. This is true for any seismic wave type and mode, including converted waves and multiples. First, the relation between τ-p transforms, plane-wave decompositions, and geometric spreading is discussed. Since an inverse τ-p transform would effectively undo the geometric spreading correction, I then give expressions to correct for anisotropic moveout in the τ-p domain for both pure-mode and converted waves. Finally, I show some synthetic and real data examples.

GEOMETRIC SPREADING CORRECTION

Spherical versus plane waves

Amplitudes of spherical waves in the t-x domain decrease with time t and propagation distance r even in a homogeneous space since the same amount of energy is spread out over an ever-increasing wavefront. In a homogeneous isotropic medium, the wavefronts originating from a point source are spheres yielding a $1/r$ amplitude decrease. However, the same wavefront may be very different from a sphere in a homogeneous anisotropic medium. For instance, the resulting wavefronts of P-waves in an elliptically anisotropic medium are ellipses, and SV-waves in VTI media may exhibit kinks and/or cusps (i.e., wavefront folding). As a consequence, amplitudes do not attenuate evenly along the wavefront, and the geometric spreading depends on the propagation direction. Geometric spreading corrections therefore require knowledge of the elastic parameters. The presence of horizontal interfaces distorts the wavefronts even further, yielding more complex corrections (Newman, 1973; Ursin, 1990; Zhou and McMechan, 2000). After geometric spreading correction, a second correction is required to remove the effect of the initial source radiation pattern, which need not be isotropic either (e.g., vertical vibrator).

A plane wave in a homogeneous medium is not distorted with increasing propagation distance/time. The energy density within each plane wave remains constant—even in the case of anisotropy. Hence, no geometric spreading correction need be applied after a PWD. Amplitudes must be corrected for the initial source radiation only. This remains true for horizontally propagating plane waves in laterally homogeneous, stratified media, although strictly speaking we are no longer dealing with plane waves but with waves characterized by a specific horizontal slowness.

A mathematical explanation can be found in the Appendix. As a quick justification, however, note that reflectivity methods use the same principle. All quantities are computed using plane waves, whereupon an inverse PWD then produces the desired exact seismograms without the need for any subsequent corrections for geometric spreading (Fryer and Frazer, 1984). Hence, a PWD removes the geometric spreading for all wave modes and types simultaneously without further work.

Plane-wave decompositions and τ-p transforms

The appropriate type of PWD depends on the source type (point or line source, explosion or vibrator), the medium (axisymmetric or not), and the data volume (3D volume or 2D line). For incomplete data volumes (e.g., a 2D line), a proper PWD is still possible under specific conditions.

I express the transient plane waves in terms of the intercept, or vertical, time τ and the horizontal slownesses p_x and p_y along the x- and y-axes, respectively.

Three-dimensional data volume and point source.—For a point source (e.g., a perfect explosion or air gun) and a complete 3D data volume, a so-called τ-p_x-p_y transform yields a perfect PWD for arbitrary anisotropy which may vary continuously or abruptly with depth. The transformed section $\mathbf{u}(\tau, p_x, p_y)$ is obtained from the original data $\mathbf{u}(t, x, y)$ by means of an integration over different slant planes, i.e.,

$$\mathbf{u}(\tau, p_x, p_y) = \iint \mathbf{u}(\tau + p_x x + p_y y, x, y)\, dx\, dy, \quad (1)$$

with $\tau = t - p_x x - p_y y$. Equation (1) is a proper slant stack in the sense that data are integrated (summed) over a slant plane described by a specific intercept time τ and slope (p_x, p_y). A uniform plane in t-x-y space is transformed to a point in τ-p_x-p_y space. The τ-p_x-p_y transform produces, as a consequence, a maximum output if a slant plane is tangent to a reflection moveout curve. In this sense, the τ-p_x-p_y transform is a contact transformation (Phinney et al., 1981). A hyperboloidal $t(x, y)$ moveout curve maps onto an ellipsoidal $\tau(p_x, p_y)$ curve. Nonhyperboloidal $t(x, y)$ moveout curves map onto anellipsoidal $\tau(p_x, p_y)$ curves. To minimize aliasing, the data volume unfortunately requires a very good spatial distribution with both offset and azimuth before geometric spreading corrections by means of a PWD become possible, thereby limiting the applicability of this approach.

Two-dimensional data line and point source.—For a point source and a 2D line of data, the conventional τ-p_x transform (the conventional or Cartesian slant stack) does not yield a proper PWD since it neglects the fact that energy actually spreads out in three dimensions whereas the integration (summation) is only over a single coordinate axis. A proper τ-p_x-p_y transform cannot be implemented because the data volume is incomplete. If we assume, however, that the medium exhibits rotational symmetry around the vertical axis, then the 2D data line is identical in all directions. The data can then be rotated over all azimuths, thereby yielding again a complete 3D data volume. PWDs based on this assumption are equivalent to the so-called cylindrical τ-p_r transforms in their diverse numerical implementations (Chapman, 1981; Brysk and McCown, 1986; Wang and Houseman, 1997). Therefore, we can automatically correct for the spherical divergence in a 1D axisymmetric medium by means of a PWD without prior knowledge of the underlying velocity model. Both laterally homogeneous, isotropic, and VTI media exhibit axisymmetry for all seismic wave modes and types.

Two-dimensional data line and line source.—By using a perfect line source of infinite length, waves are forced to propagate in a 2-D plane perpendicular to the source since the wavefield is invariant along the source direction. This remains true even for converted waves. Hence, application of a conventional τ-p_x transform (for a line source in the y-direction) yields a perfect PWD for arbitrary anisotropy. The conventional τ-p_x transform is given by

$$\mathbf{u}(\tau, p_x) = \int \mathbf{u}(\tau + p_x x, x)\, dx, \quad (2)$$

with $\tau = t - p_x x$. A uniform line in t-x space is transformed to a point in τ-p_x space, and a hyperbolic $t(x)$ moveout curve maps onto an elliptic $\tau(p_x)$ curve (Phinney et al., 1981; Schultz, 1982).

Unfortunately, actual seismic sources are better described by a point source than a line source. On the other hand, for an axisymmetric medium, it is possible to transform point-source data to equivalent line-source data by means of lateral filtering (Wapenaar et al., 1992). After lateral filtering, the application of a conventional τ-p_x transform [equation (2)] yields the desired PWD. The advantage of lateral filtering is that the integration coefficients depend on offset only and can by applied on all time samples within a trace simultaneously, thereby yielding a very efficient integration algorithm. Wapenaar et al. (1992) also outline the required integration procedures for vibroseis data with horizontal sources (e.g., nine-component data). Special treatment for these sources is required because horizontal point forces break the rotational symmetry around the vertical axis.

Therefore, geometric spreading can be removed in laterally homogeneous media in a straightforward way by a PWD without any knowledge of the underlying velocity model. Restrictions on the symmetry type of anisotropy that can be handled depend in practice only on the acquisition geometry and data volume (three dimensional or two dimensional). The subsequent moveout correction and stacking must also be done in the τ-p domain since an inverse τ-p transform would reconstruct the geometric spreading. Naturally, knowledge of the underlying velocity model is required for the moveout corrections.

MOVEOUT CORRECTIONS AND STACKING IN THE τ-p DOMAIN

Moveout corrections and NMO stretch

To compute the moveout corrections in the τ-p domain, we first need an expression for the $\tau(p)$ curves. In the following, I use $\tau(p)$ to denote $\tau(p_x, p_y)$, $\tau(p_r)$, or $\tau(p_x)$, respectively, depending on the appropriate free parameter and τ-p transform. The radial slowness p_r is defined by $(p_x^2 + p_y^2)^{1/2}$.

Van der Baan and Kendall (2003) show that the interval $\Delta\tau_i(p)$ curve in each layer i is given by

$$\begin{aligned}\frac{\Delta\tau_i}{\Delta\tau_{0,i}} &= \frac{\grave{v}_{0,i}\acute{v}_{0,i}}{\grave{v}_{0,i} + \acute{v}_{0,i}}[\grave{q}_{z,i} + \acute{q}_{z,i}] \\ &= \frac{\grave{v}_{0,i}\acute{v}_{0,i}}{\grave{v}_{0,i} + \acute{v}_{0,i}}\left[\left(\grave{v}_{ph,i}^{-2} - p_r^2\right)^{1/2} + \left(\acute{v}_{ph,i}^{-2} - p_r^2\right)^{1/2}\right]. \quad (3)\end{aligned}$$

The total $\tau_i(p)$ curve consists of a summation over all interval $\Delta\tau_i(p)$ curves, i.e.,

$$\tau_n(p) = \sum_{i=1}^{n} \Delta\tau_i(p). \quad (4)$$

In expression (3), $\grave{q}_{z,i}$ and $\acute{q}_{z,i}$ represent the vertical slowness of, respectively, the down- and upgoing plane waves in layer i, $\grave{v}_{ph,i}$ is the phase velocity of the downgoing wave, and $\grave{v}_{0,i}$ is the associated vertical plane-wave velocity. Equation (3) is valid in a laterally homogeneous earth for all seismic modes (i.e., P, SV, SH), including any converted waves and for arbitrary anisotropy. For pure-mode waves propagating in anisotropic layers with a horizontal symmetry plane (e.g., VTI anisotropy), expression (3) simplifies to (Van der Baan and Kendall, 2002)

$$\Delta\tau_i = \Delta\tau_{0,i}\frac{v_{0,i}}{v_{ph,i}}\left[1 - p_r^2 v_{ph,i}^2\right]^{1/2}. \quad (5)$$

This equation is reminiscent of the elliptical equation for interval $\Delta\tau_i(p)$ curves in isotropic media (Schultz, 1982). Hence, a hyperbolic moveout curve in t-x space maps onto an elliptic moveout curve in τ-p space. Furthermore, nonhyperbolic $t(x)$ moveout curves yield anelliptic $\tau(p)$ curves (Van der Baan and Kendall, 2002, 2003). Up- and downgoing waves of identical mode have the same phase velocity in VTI media because of the presence of a horizontal symmetry plane. The acute and grave accents on the phase velocity $v_{ph,i}(p_x, p_y)$ are therefore omitted in expression (5).

To describe the $\tau(p)$ curves, we now only need expressions for the phase velocities in terms of the horizontal slowness, i.e., $\grave{v}_{ph,i}(p_x, p_y)$ and $\acute{v}_{ph,i}(p_x, p_y)$ for down- and upgoing waves, respectively. Van der Baan and Kendall (2002 and 2003) derive both exact and reduced-parameter expressions for the phase velocities in transversely isotropic media with a horizontal axis of symmetry (HTI) and for VTI media. The reduced-parameter expressions are needed to render the problem of anisotropy–parameter estimation more unique and thereby more stable. It was shown that P-waves in VTI media are well described by

$$\tilde{v}_P^2(p_r) \approx \alpha_n^2 \frac{1 - 2\eta\alpha_n^2 p_r^2}{1 - 2\eta\alpha_n^2 p_r^2 - 2\eta\alpha_n^4 p_r^4}, \tag{6}$$

with α_n the P-wave stacking velocity and η an anisotropy parameter. Expression (6) is not a good approximation to the exact P-wave phase velocities unless used in combination with equations (3) and (5) describing the form of the $\tau(p)$ curves and $v_{0,i} = \alpha_{n,i}$. In addition, the expression is unstable for slownesses beyond the maximum horizontal slowness, i.e., for $p_r > \alpha_n^{-1}(1+2\eta)^{-1/2}$.

Furthermore, for SV-waves in VTI media,

$$\tilde{v}_{SV}^2(p_r) \approx \beta_n^2 \frac{-1 + 2\sigma\left(\beta_n^2 p_r^2 - 1\right) + \left\{\left(-1 + 2\sigma\left(\beta_n^2 p_r^2 - 1\right)\right)^2 + 8\sigma\beta_n^4 p_r^4\right\}^{1/2}}{4\sigma\beta_n^4 p_r^4}, \tag{7}$$

with β_n the SV-wave stacking velocity and σ an anisotropy parameter. Contrary to equation (6), expression (7) is a first-order approximation. Hence, it works best for small anisotropy (i.e., small σ). Equation (6), on the other hand, describes the kinematic behavior of the P-waves and therefore provides very accurate results even for large anisotropy (i.e., for large η). If the denominator in equation (7) approaches zero, $\tilde{v}_{SV}$ converges to $\beta_n(1+2\sigma)^{-1/2}$. Furthermore, $v_{0,i} = \beta_n(1+2\sigma)^{-1/2}$ in expressions (3) and (5).

The anisotropy parameters η and σ can be expressed in terms of the Thomsen parameters δ and ε (Thomsen, 1986; Tsvankin and Thomsen, 1994; Alkhalifah and Tsvankin, 1995), and they equal zero for either isotropic or elliptically anisotropic media.

The required anisotropy parameters and stacking velocities for the moveout corrections can be estimated in a variety of ways. For instance, they can be obtained using modified Taylor series expressions and a semblance analysis (Alkhalifah, 1997) or by directly picking and fitting moveout curves in the τ-p domain (Van der Baan and Kendall, 2002). The former method tends to be simpler in practice, while the latter is more accurate on good-quality data. However, the two approaches can also be combined. The moveout curves can be estimated in the t-x domain using either a semblance analysis or by picking traveltimes. Next, a modified Taylor series curve is fitted to the estimated moveout curve. The fitted curve is then transformed to the τ-p domain where the required anisotropy parameters are estimated (Wookey et al., 2002). The latter method has the advantage that velocities and anisotropy parameters can be estimated quite conveniently without the need to introduce any radical changes to the conventional processing stream of picking velocities in the time-offset domain.

Note, however, that large trade-offs exist between the obtained stacking velocities and anisotropy parameters unless large offset–depth ratios are available ($x/z > 2$) (Alkhalifah, 1997; Wookey et al., 2002). On the other hand, this is unimportant if we only wish to flatten the gathers, that is, if exact knowledge of the underlying anisotropy parameters is less relevant.

Similar to the conventional t-x domain approach, a moveout correction in the τ-p domain amounts to flattening the $\tau(p)$ curves. However, contrary to an t-x moveout correction,

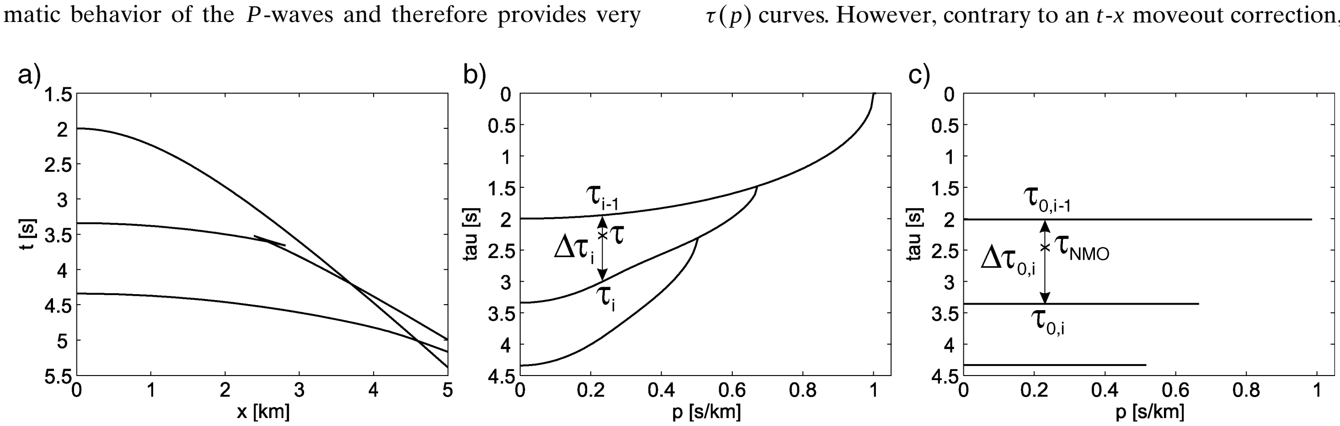

Figure 1. Moveout correction in the τ-p domain. A t-x CMP gather (a) is mapped to the τ-p domain (b). Reflections no longer cross and the triplication is unfolded. A moveout correction is then done by flattening the τ-p curves (c) and stacking over slowness. This amounts to linearly stretching the sequence $\Delta\tau_i(p)$ to a length equal to the interval zero-intercept time $\Delta\tau_{0,i}$. Thus, a point at $\tau(p)$ is moved downward to $\tau_{NMO}(p)$ after moveout correction.

the $\tau(p)$ curves are moved downward with intercept time. On the other hand, reflections do not cross in the τ-p domain, and triplications (cusps) are unfolded (Figure 1). Hence, theoretically at least, it becomes possible to stack triplications in this domain. In practice, the NMO stretch is often too large unless triplications occur near the vertical axis. In the latter case we would first deal with the unusual phenomenon of wavelet compression.

If the stacking velocities and anisotropy parameters are assumed to be constant within each individual layer, then a moveout correction in the τ-p domain amounts to linearly stretching each interval time sequence $\Delta\tau_i(p)$ to a length equal to the zero-offset interval intercept time $\Delta\tau_{0,i}$ (Figures 1b and 1c). Hence, NMO stretch (Dunkin and Levin, 1973) occurs in both the t-x and τ-p domains. In the latter domain, it is given by

$$stretch_i(p) = \frac{\Delta\tau_{0,i}}{\Delta\tau_i(p)}, \tag{8}$$

and ranges therefore from one [0%] to infinity for conventional situations. Values less than one (wavelet compression) only occur if a triplication is centered around the vertical axis. For isotropic media, it is quite simple to express this equation directly in terms of the zero-offset traveltime $t_{0,i}$, the offset (x, y), and the rms velocity. This is much harder for anisotropic media, although it remains straightforward to compute the actual stretch using formula (8) while correcting for the moveout layer by layer.

From a comparison of Figures 1b and 1c, one can easily deduce how the moveout-corrected intercept time $\tau_{NMO}(p)$ is computed for a given intercept time $\tau(p)$. However, as a result of the stretching and the possible occurrence of gaps in the time sequence, it is better to calculate the original intercept time $\tau(p)$ corresponding to a given $\tau_{NMO}(p)$. Thus, within layer i,

$$\tau^{(i)}(\tau_{NMO,i}) = \tau_{i-1} + \frac{(\tau_{NMO,i} - \tau_{0,i-1})}{stretch_i}. \tag{9}$$

Within each layer, $\tau_{NMO,i}(p)$ ranges from $\tau_{0,i-1}$ to $\tau_{0,i}$, and $\tau^{(i)}(p)$ ranges from $\tau_{i-1}(p)$ to $\tau_i(p)$. The last two intercept times define the lower and upper bounds within layer i [equation (4)]. Hence, τ-p domain-based moveout correction is analogous to layer stripping in that it is done layer by layer and for each slowness separately. Note that expressions (8) and (9) are valid for arbitrary anisotropic strength and symmetry.

Some important differences exist between NMO stretch in the t-x and τ-p domains. Equation (8) clearly indicates that the actual NMO stretch varies from layer to layer, independent of the elastic parameters in the shallower layers. Hence, while in one particular layer the NMO stretch may exceed a predefined threshold, this is not necessarily true for the deeper layers. Examples include the presence of velocity reversals (i.e., low-velocity layers) and near cusps of SV-waves in strongly anisotropic media (i.e., between inflection points on the slowness sheets). Unfortunately, this complicates the implementation.

The band-limited nature of the data should also be taken into account while applying a mute. A time taper of approximately the principal period of the reflections needs to be applied while muting the data beyond a predefined amount of stretch. It remains naturally possible to apply a mute after moveout correction to remove any unwanted artifacts, including NMO stretch.

Stacking

Stacking in the time-offset domain is a very simple process since it involves only a horizontal summation of amplitudes of moveout-corrected data $\mathbf{u}_{mo}(t, x, y)$ over all available offsets and azimuths. Intuitively, we would expect that stacking in the τ-p domain involves a horizontal summation over slowness (Stoffa et al., 1981, 1982). However, stacking over offset is a partial forward τ-p transform where we map the moveout-corrected data onto intercept times corresponding to zero horizontal slowness. Similarly, stacking over slowness includes many aspects of an inverse τ-p transform. Hence, we need to apply time differentiation to compensate for the loss of resolution attributable to the stacking in analogy with proper inverse τ-p transforms. It is not a complete inverse transform because the integration over varying intercept times is left out—that is, we recover the zero-offset stacked trace only. Furthermore, it does not reconstruct the geometric spreading because of the moveout corrections and because it is an incomplete transform. Again, the actual procedure depends on the data volume.

Three-dimensional data volume.—Stacking over offset of 3D data is mathematically described by

$$\mathbf{u}_{stack(t,x,y)}(t) = \iint \mathbf{u}_{mo}(t, x, y)\, dx\, dy. \tag{10}$$

Inspection of expressions (1) and (10) clearly shows that the latter corresponds to a partial forward τ-p_x-p_y transform where we compute the zero-slowness trace only.

The inverse τ-p_x-p_y transform for a 3D data volume is given by (Chapman, 1981; Brysk and McCown, 1986)

$$\mathbf{u}(t, x, y) = -\frac{1}{4\pi^2}\frac{d^2}{dt^2}\iint \mathbf{u}(t - p_x x - p_y y,\, p_x,\, p_y)\, dp_x\, dp_y. \tag{11}$$

The double time differentiation arises from the change of variables in the inverse Fourier transform [see expression (A-2)] and is required to compensate for the enhancement of low-frequency amplitudes during stacking (Phinney et al., 1981).

If stacking in the t-x-y domain corresponds to a partial forward τ-p_x-p_y transform to compute the zero-slowness trace, then stacking in the τ-p_x-p_y domain corresponds to calculating the zero-offset trace using a partial inverse τ-p_x-p_y transform. Therefore, the correct stacking equation is

$$\mathbf{u}_{stack(\tau,p_x,p_y)}(\tau) = -\frac{1}{4\pi^2}\frac{d^2}{d\tau^2}\iint \mathbf{u}_{mo}(\tau,\, p_x,\, p_y)\, dp_x\, dp_y, \tag{12}$$

where the double time differentiation plays an identical role as before. It only needs to be applied once on every stacked trace.

Two-dimensional data line.—Stacking of 2D data is mathematically described by

$$\mathbf{u}_{stack(t,x)}(t) = \int \mathbf{u}_{mo}(t, x)\, dx. \tag{13}$$

A comparison with equation (2) reveals that we are dealing with a partial forward Cartesian τ-p_x transform to derive the zero-slowness trace. Stacking 2D data does not try to emulate a 3D stack response by invoking axisymmetry of the data. This would lead to a weighting factor equal to the offset x in the integration (13)—analogous with the zero-slowness forward cylindrical τ-p_r transform (Brysk and McCowan, 1986). On the contrary, it assumes the presence of a line source. As a consequence, we only need to deal with the inverse τ-p_x transform given by (Chapman, 1981; Brysk and McCowan, 1986)

$$\mathbf{u}(t, x) = -\frac{1}{2\pi}\frac{d}{dt}H\int \mathbf{u}(t - p_x x,\, p_x)\, dp_x, \qquad (14)$$

regardless of whether we have line or point source data. Hence, the correct expression for stacking over slowness is

$$\mathbf{u}_{stack(\tau,p_x)}(\tau) = -\frac{1}{2\pi}\frac{d}{d\tau}H\int \mathbf{u}_{mo}(\tau,\, p_x)\, dp_x. \qquad (15)$$

The Hilbert transform H causes a 90° phase rotation of the data and corrects for the phase rotation introduced by the time differentiation. Again, both operators need to be applied on stacked traces only and compensate for loss of resolution during stacking.

The time variable in the stacked traces $\mathbf{u}_{stack(t,x)}$ and $\mathbf{u}_{stack(\tau,p_x)}$ [expressions (13) and (15)] simultaneously equal the arrival time t and the intercept time τ. Both stacked sections can be directly compared. In practice, the two stacked traces are highly similar but not identical—even if the geometric spreading of the $t(x)$ trace has been corrected accurately. Some differences occur, for instance, because the head waves map onto the $\tau(p)$ moveout curves. They therefore contribute constructively to the amplitudes of the $\tau(p)$ stacked traces, whereas this is not the case for the conventional $t(x)$ stacked traces. The same remark holds for stacked traces resulting from 3D data volumes [expressions (10) and (12)]. The advantages of τ-p domain processing lie in the automatic removal of geometric spreading and in the fact that the τ-p transform acts as a dip filter, thereby limiting the influence of several types of noise.

EXAMPLES

Synthetic data example

First, a synthetic example is considered. This particular three-layer model is used in Van der Baan and Kendall (2002, 2003) and is composed of an uppermost isotropic layer ($\alpha_{n,1} = 2$ km/s, $\beta_{n,1} = 1$ km/s), an anisotropic shale (VTI), and again an isotropic layer ($\alpha_{n,3} = 4$ km/s, $\beta_{n,3} = 2$ km/s). Each layer has a thickness of 1 km and a constant density of 2 g/cm^{-3}. Underneath the three-layer model is an isotropic half-space ($\alpha_{n,4} = 5$ km/s, $\beta_{n,4} = 2.5$ km/s, density = 2.5 g/cm^{-3}). The elastic parameters of the anisotropic shale are taken from Thomsen (1986) and are displayed in Table 1. Figure 4 in Van der Baan and Kendall (2003) displays the slowness and wave sheets of the anisotropic shale.

The synthetic sections are created by means of generalized ray tracing (Fuchs and Müller, 1971) extended to VTI media using the methodology for computing reflection and transmission coefficients outlined in Fryer and Frazer (1984), combined with analytical expressions for the stress and displacement vectors given by Fryer and Frazer (1987). Generalized ray tracing involves a partial ray expansion combined with an integration over real slowness (Chapman and Orcutt, 1985). It leads to exact waveforms, including phase changes and head waves, and has the advantage over reflectivity methods that solely specific predefined arrivals are computed. In this case only the primary reflections and their head waves are calculated.

Figure 2a shows the three primary P-P reflections and the first head wave resulting from an explosive point source. A gradual phase rotation is visible in the first reflection after it splits from the head wave around 1.5 km. Figure 2b displays the same data transformed to the τ-p domain by first applying lateral filtering and then a Cartesian τ-p_x transform. The head wave has mapped onto a single point—namely, the critical slowness of the first reflection ($p = 0.27$ s/km). This explains the strong increase in the amplitude at this point. Similar sudden increases of the amplitudes in the $\tau(p)$ moveout curves of the other reflections are not visible because the head waves were not yet present in the limited-offset shot gather (Figure 2a). Longer offsets would have been needed to detect and map them into the τ-p gather.

To demonstrate that the geometric spreading has indeed been automatically corrected, I compare the zero-offset trace after a t-x–based geometric spreading correction and the zero-slowness trace in Figure 2b after time differentiation. The resulting zero-slowness trace should be equal to the zero-incidence total reflection coefficients (including transmission effects) convolved with the source wavelet. The resulting zero-offset trace equals to first order the same convolution of total reflection coefficients and source wavelet. Small discrepancies may occur because neighboring points on the reflectors (and thereby neighboring reflection coefficients) also influence the amplitude recorded at zero incidence on account of the Fresnel zone.

Figure 3 displays the resulting zero-offset and zero-slowness traces. The geometric spreading has been corrected using expressions in Zhou and McMechan (2000). The two traces are nearly identical, indicating that the geometric spreading has indeed been removed for the $\tau(p)$ traces near zero slowness. Only some minor differences occur. The small wavelets around the first and second reflections are caused by integration artifacts in the way the synthetics are created. They map onto different points in τ-p space and are therefore absent in the $\tau(p)$ trace. The high-frequency oscillations around the third reflection are from the time differentiation and can be removed by a simple high-cut frequency filter.

Table 1. Elastic parameters of the shale used in the numerical examples. All values are taken from Thomsen (1986).

Parameter	Value
α_0	3.048 (km/s)
β_0	1.490 (km/s)
ε	0.255
δ	−0.050
η	0.339
σ	1.276

As a second test, I extract the total reflection coefficients along the $\tau(p)$ curves in Figure 2b and compare them with the theoretical ones. The latter are computed using the approach described in Fryer and Frazer (1984, 1987). Figure 4 displays both the extracted and exact total reflection coefficients. The two are again highly similar, indicating that the geometric spreading of all arrivals in the τ-p domain has indeed been corrected automatically at all slownesses. The abrupt change in the reflection coefficient of the first reflection around $p = 0.27$ s/km is a result of the head wave being mapped to approximately a single point. Similarly, the drop-off of the recovered reflection coefficients of the other reflections at larger slownesses is because of the finite lateral extent of the synthetic shot gather, as explained previously.

As a final demonstration that τ-p domain stacking is a powerful tool, I create a synthetic SV-wave shot gather. A fictitious explosive point source is used with an isotropic radiation pattern for the SV-waves. Figure 5a contains the resulting $t(x)$ gather for the primary pure-mode reflections and their head waves. A comparison with Figure 2a shows that the behavior of pure-mode SV-waves is significantly more complex than that of pure-mode P-waves. Several polarity reversals are visible, and each reflection gives rise to two head waves: a head wave that propagates as a P-wave along the interface and another one that propagates as an SV-wave. These separate, for instance, from the first reflection around offsets of 1 and 2.5 km, respectively. Finally, a triplication is visible in the second reflection around 2.5 km. For reference, Figure 1a displays the ray theoretical $t(x)$ reflection moveout curves.

While the actual time-offset gather looks surprisingly complex, the resulting $\tau(p)$ gather after lateral filtering and the τ-p_x transform is reassuringly simple (Figures 1b and 5b). Again, all head waves map onto single points. We can clearly distinguish

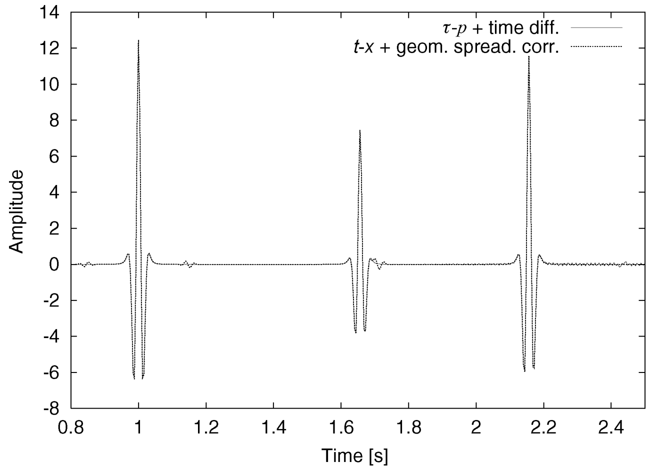

Figure 3. Comparison of the zero-offset trace after a t-x–based geometric spreading correction and the zero-slowness trace of the τ-p gather after time differentiation. The two traces are nearly identical, indicating that the geometric spreading in the τ-p domain has been removed for small slownesses. No Hilbert transform is applied since the 90° phase rotation is already included in the lateral filtering technique.

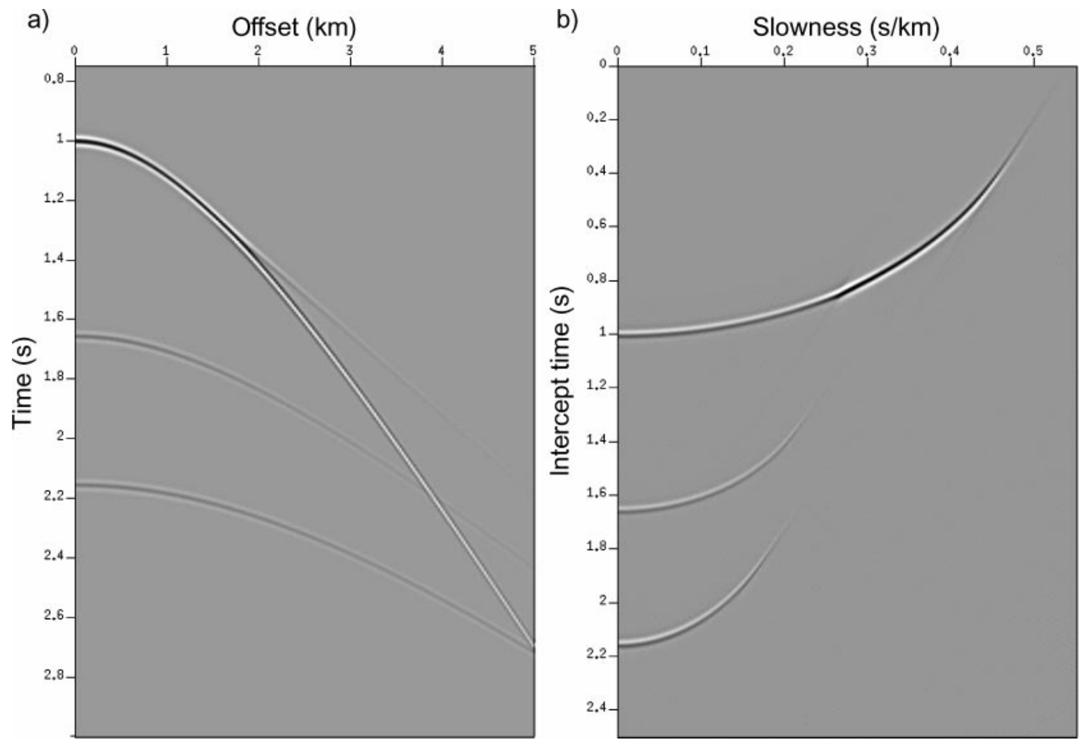

Figure 2. (a) P–P primary reflections plus head wave for the considered synthetic model. The amplitudes are scaled with time squared for display purposes. (b) Resulting τ-p gather after lateral filtering and a conventional τ-p_x transform. The head wave has mapped onto a single point and can therefore be stacked.

the three individual reflections because events no longer overlap and the triplication is unfolded. Now, we can stack the triplication, and the head waves can contribute to the stacked sections, thereby potentially increasing stack quality.

In practice, it may be difficult to stack the triplication far beyond the first inflection point in the τ-p domain (i.e., beyond the first cusp in the time-offset domain) because of the NMO stretch. Indeed, the interval intercept time $\Delta\tau_i(p)$ quickly diminishes beyond this point (compare Figures 1b and 5b with Figure 1c). In addition, for this particular model, the reflection coefficients between the two inflection points are very small, thereby limiting the final contribution to the stacked section even further.

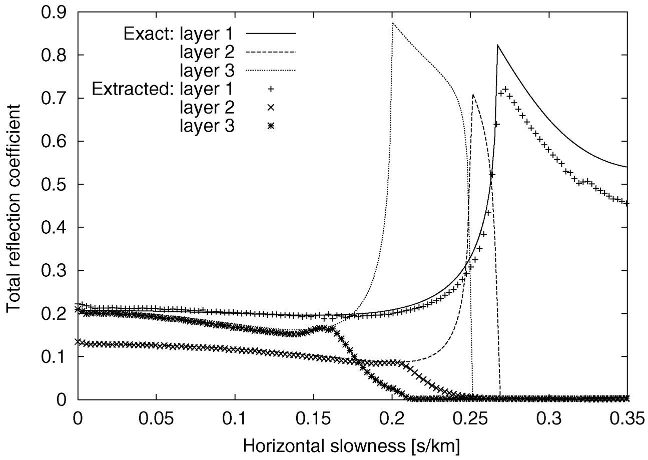

Figure 4. Exact and extracted total reflection coefficients from the τ-p gather. Their high similarity demonstrates that the geometric spreading has been correctly removed for all slownesses.

Nonetheless, we can conclude that stacking in the τ-p domain is a very powerful tool. The geometric spreading of all wave modes and types is automatically removed, nonhyperbolic moveout resulting from layering is taken into account, reflections no longer cross, triplications are unfolded, and even head waves can contribute constructively to the stacked sections. In addition, the τ-p transform acts as a dip filter, thereby limiting the influence of certain types of noise such as surface waves.

Real data example

For this real 2D data example, I use a data set acquired in a relatively flat part of the Western Canadian sedimentary basin using a 5.5-km static spread with a group interval of 20 m and a shot interval of 80 m (Kendall and Pullishy, 2002). The trace spacing in the CMP gathers was very irregular. As a consequence, the CMP-sorted data after lateral filtering were dominated by aliasing artifacts. The proposed processing methodology was therefore applied on the common-shot gathers instead of attempting to solve this inconvenience by means of trace

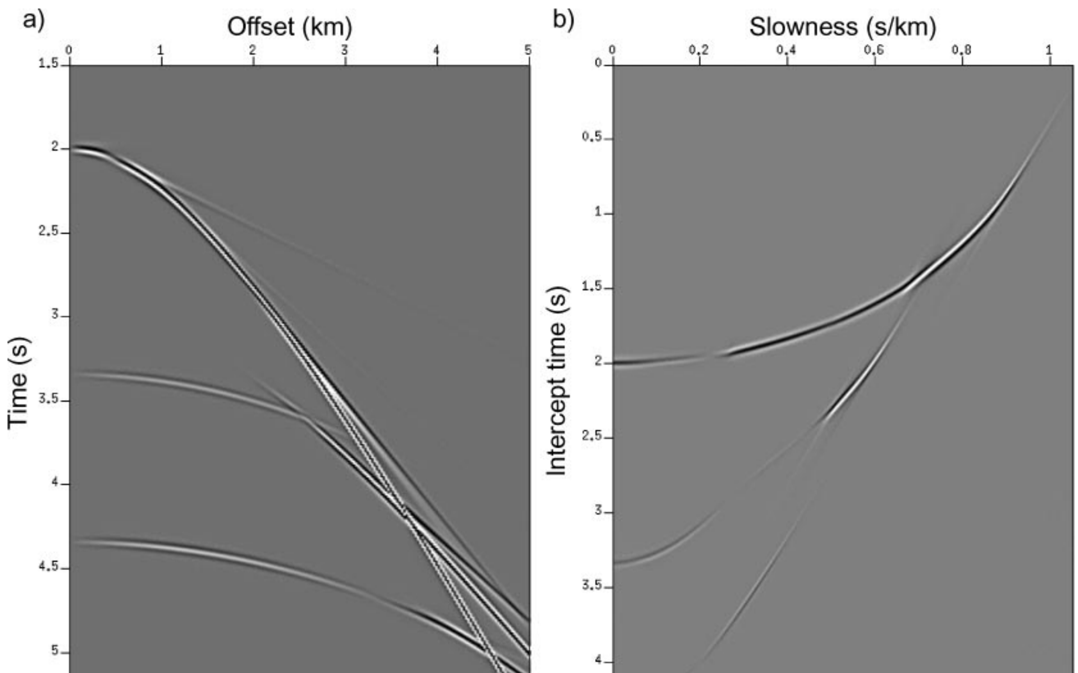

Figure 5. (a) SV–SV primary reflections plus head waves for the same synthetic model. Note the triplication in the second reflection near 2.5 km. Amplitudes have again been scaled with time squared for display purposes. (b) Resulting τ-p gather after lateral filtering and a τ-p_x transform. Reflections no longer cross, the triplication has been unfolded, and head waves are mapped onto single points. This gather, is much simpler than the original t-x gather, and both the triplication and the head waves can now contribute constructively to the stacked section. Compare with Figures 1a and 1b, which display the ray theoretical $t(x)$ and $\tau(p)$ moveout curves.

interpolation with corresponding problems. This renders the described techniques less ideal for the particular data set in question. Nevertheless, it still serves as a good illustration of its applicability and as a real data comparison.

The processing stream was kept basic. It consisted of a top mute to remove head waves and other linear events in the far offset, band-pass filtering to remove ground roll and high-frequency noise, f-x spatial-prediction filtering to increase the S/N ratio, and minimum-phase predictive deconvolution to boost the frequency content. Refraction statics were also applied. The resulting t-x stacked section after geometric spreading correction is displayed in Figure 6a. The technique of Ursin (1990) was used to remove the geometric spreading.

Next, lateral filtering was applied on the processed gathers before geometric spreading corrections, the resulting data were transformed to the τ-p domain and stacked. Finally, time differentiation was applied on the stacked traces to compensate for the loss of frequency content during stacking. The antialiasing filter of Moon et al. (1986) was applied to reduce aliasing in the τ-p transform. Figure 6b displays the final result. The same isotropic velocity model was used to obtain both stacked sections. Some reflectors displayed small amounts of nonhyperbolic moveout. However, this was most prominent after the NMO stretch cut-off and therefore was neglected.

A comparison of Figures 6a and 6b shows highly similar stacked sections. The individual reflectors have approximately the same strength in both stacked sections, indicating that geometrically spreading has been correctly removed in both approaches. However, the relative strength of, in particular, the first few reflectors would have been quite different if the head waves had not been muted out in the far offset. The overall quality of both stacked sections is identical except for the uppermost part. The quality of the $\tau(p)$ stacked traces is slightly higher here because the τ-p transform acts as a dip filter, thereby removing some remnant surface wave energy that still contaminates the $t(x)$ stacked traces. The ringing in the 36th stacked trace resulting from some bad traces has been reduced for the same reason.

DISCUSSION

The described methodology is in many ways more flexible than the conventional approach of removing geometric spreading and stacking amplitudes in the time-offset domain. The geometric spreading of all wave modes and types is automatically and jointly removed, nonhyperbolic moveout resulting from layering is taken into account, reflections no longer cross, triplications are unfolded, and even head waves can contribute constructively to the stacked sections. In addition, the τ-p transform acts as a dip filter, thereby limiting the influence of certain types of noise such as surface waves.

Both the PWD and the conventional geometric spreading corrections rely on the presence of a laterally homogeneous

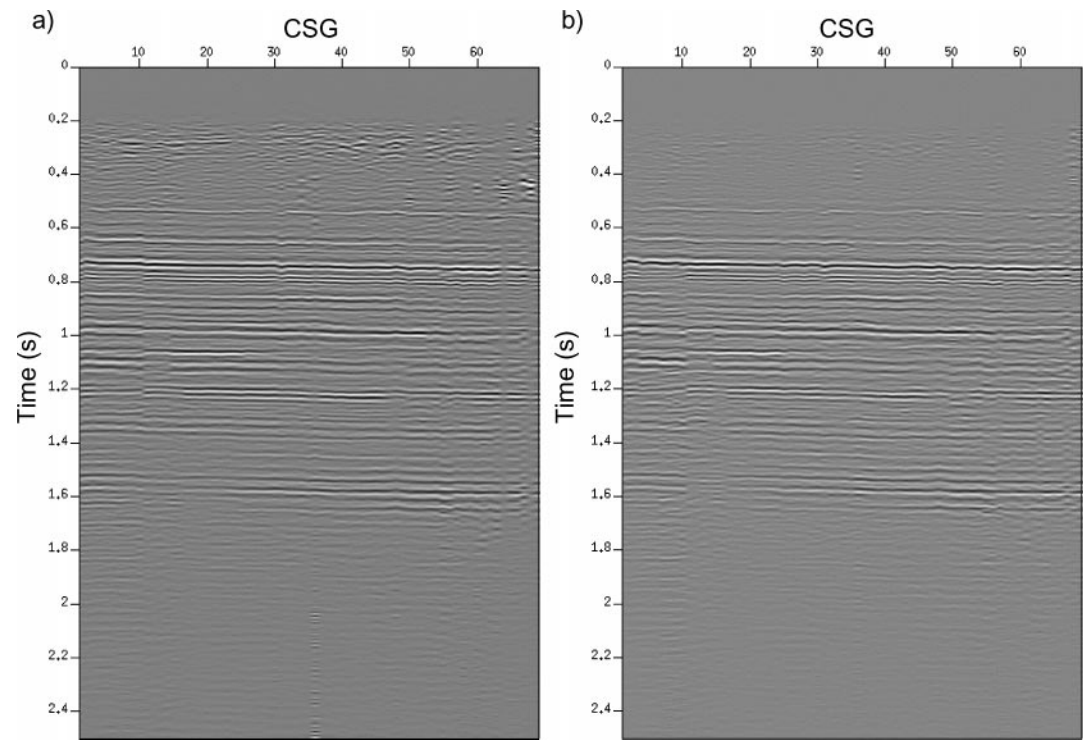

Figure 6. Comparison of stacking techniques on real data. (a) Conventional t-x stacked section after geometric spreading correction. (b) The τ-p stacked section after PWD to remove spherical divergence. The two stacked sections are highly similar except at small two-way traveltimes. The τ-p section has here a higher S/N ratio because the τ-p transform acts as a dip filter. The maximum stretch mute was limited to 50% in both cases.

earth. The real earth is not one dimensional. However, this problem is reduced by applying the proper τ-p transform on CMP or common conversion-point sorted data (Wapenaar et al., 1992).

An inconvenience of the PWD approach is that a good spatial distribution with both azimuth and offset is an absolute prerequisite for the method to work for 3D acquisition geometries. Otherwise, the data will be dominated by aliasing artifacts after a PWD. For 2D receiver lines a good regular distribution with offset is needed. In addition, the method requires that the medium be axisymmetric. That is, the method here is limited to 1D media (isotropic or VTI). If the actual medium deviates from these conditions, then the method will most probably still yield a good first-order correction.

Some high-frequency noise may be introduced by the required time differentiation of the stacked traces, particularly for short traces. A simple high-cut frequency filter will remove the undesired artifacts in most cases. However, if significant noise is introduced by the time differentiation, a 90° phase rotation may suffice for a comparison with a 2D $t(x)$ stacked section. This comes, however, at the expense of some loss in high-frequency content.

Both τ-p and t-x moveout corrections can handle exactly the effect of a single dipping layer as long as data are sorted in the CMP domain. However, both break down in the presence of more complicated moderate-to-strong lateral inhomogeneities. Stacking and processing in the τ-p domain therefore has several potential advantages over the conventional t-x approach. It relies otherwise on the same assumptions as more conventional techniques.

CONCLUSIONS

Plane waves in laterally homogeneous media are not subject to geometric spreading. Hence, the geometric spreading can be removed simultaneously for all wave modes and types without any prior knowledge of the actual underlying velocity field by applying a plane-wave decomposition. The required plane-wave decomposition, i.e., τ-p transform, depends on the actual acquisition geometry and source type. Subsequent moveout correction and stacking is also done in the τ-p domain since an inverse τ-p transform would reconstruct the geometric-spreading correction. The proposed methodology is exact for dense 3D data volumes and arbitrary anisotropy in laterally homogeneous media or for 2D data lines in a 1D, isotropic, or VTI medium. The resulting stacked section can be used for any poststack processing such as time migration.

ACKNOWLEDGMENTS

The author thanks Veritas GeoServices, Calgary, for permission to use this data set and Shell Expro UK for financial support. Rob Kendall is thanked for providing the data set in a rather specific format and for determining and applying the refraction statics. The manuscript benefitted from discussions with both Rob and Mike Kendall. Kees Wapenaar kindly answered questions about lateral filtering. Finally, I am thankful to Jeroen Goudswaard, who first mentioned lateral filtering to me, and to Rob Ferguson, Vladimir Grechka, Bjørn Ursin, and an anonymous reviewer for their comments and suggestions. Bjørn Ursin suggested comparing the zero-offset and zero-slowness traces.

APPENDIX

PLANE WAVES, GEOMETRIC SPREADING, AND PROPER τ-p TRANSFORMS

Geometric spreading of spherical waves.—The relative geometric spreading of a wavefront is computed by considering the relative changes over time in the area spanned by a ray tube. If we assume that the energy remains constant over time (i.e., no attenuation, reflection, or transmission losses), then the same amount of energy is spread out over an ever-increasing area for an expanding wavefront. An absolute value for the geometric spreading is obtained by normalizing the relative spreading using the velocity around the source, i.e., with the initial curvature. This idea is used by Newman (1973) and Ursin (1990) to compute their expressions for the geometric spreading in the t-x domain in a laterally homogeneous, isotropic medium and can be traced back to Gutenberg (1936).

Plane-wave decompositions and τ-p transforms.—To demonstrate that a proper τ-p transform is a plane-wave decomposition and that the resulting plane waves are not subject to geometric spreading in a laterally homogeneous medium, I consider the particle displacement field $\mathbf{u}(t, x, y, z)$ as caused by a point source at an arbitrary position and assume that it is the solution to the linear wave equation (i.e., finite amplitude waves in a noiseless environment).

First, a forward 3D Fourier transform over time and position is applied on the wavefield as recorded on a plane defined by $z = z_r$. The change of variables $k_x = \omega p_x$ and $k_y = \omega p_y$ is used, with ω the circular frequency and k_x and k_y the horizontal wavenumbers. This leads to

$$\mathbf{u}(\omega, p_x, p_y, z_r) = \iiint \mathbf{u}(t, x, y, z_r) e^{-i\omega(p_x x + p_y y - t)}\, dx\, dy\, dt. \quad \text{(A-1)}$$

Using the same change of variables, the inverse Fourier transform is defined by

$$\begin{aligned} \mathbf{u}(t, x, y, z_r) &= \frac{1}{(2\pi)^3} \iiint \mathbf{u}(\omega, k_x, k_y, z_r) \\ &\quad \times e^{i(k_x x + k_y y - \omega t)}\, dk_x\, dk_y\, d\omega \\ &= \frac{1}{(2\pi)^3} \iiint \omega^2 \mathbf{u}(\omega, p_x, p_y, z_r) \\ &\quad \times e^{i\omega(p_x x + p_y y - t)}\, dp_x\, dp_y\, d\omega. \quad \text{(A-2)} \end{aligned}$$

Physically, equation (A-2) can be interpreted as a superposition of monochromatic plane waves, with wavefronts defined by $k_x x + k_y y - \omega t = constant$ or $p_x x + p_y y - t = constant$. The Fourier expansion coefficients $\mathbf{u}(\omega, k_x, k_y, z_r)$ and $\mathbf{u}(\omega, p_x, p_y, z_r)$ are weighting functions that determine the contribution of each plane wave to the complete elastic wavefield. These plane waves are purely horizontally propagating since the vertical slowness q_z is absent in the integration.

To demonstrate that a proper τ-p transform is a plane-wave decomposition, I apply an inverse Fourier transform over frequency on equation (A-1), change the order of integration, and use the equality $\int \exp[i\omega(t - p_x x - p_y y - \tau)]\, d\omega = \delta(t - p_x x - p_y y - \tau)$, where δ represents the Dirac delta function. This leads to (Chapman, 1981)

$$\mathbf{u}(\tau, p_x, p_y, z_r) = \iiiint \mathbf{u}(t, x, y, z_r) \times e^{-i\omega(p_x x + p_y y - t)}\, dx\, dy\, dt e^{-i\omega\tau}\, d\omega = \iint \mathbf{u}(\tau + p_x x + p_y y, x, y, z_r)\, dx\, dy. \quad \text{(A-3)}$$

Expression (A-3) [equation (1)] is therefore a proper PWD for a 3D wavefield recorded as a result of a point-source excitation because the forward Fourier transform [equation (A-1)] is already a PWD. However, these are not monochromatic but transient plane waves because of the inverse Fourier transform over frequency. We can also deduce from expression (A-3) that $\mathbf{u}(\tau, p_x, p_y, z_r)$ are the expansion coefficients of horizontally propagating plane waves. In a similar way, we can demonstrate that the τ-p_x and τ-p_r transforms are proper PWDs for 2D data lines recorded from a line and point source, respectively (Chapman, 1981).

Geometric spreading of plane waves.—The resulting plane waves are not subject to geometric spreading in laterally homogeneous media because these waves are propagating horizontally. The shape of these plane wavefronts are determined by Snell's law. In particular, their angle with the vertical axis in, respectively, the x-z and y-z planes is defined by $\sin\theta_x = p_x v_{ph}$ and $\sin\theta_y = p_y v_{ph}$. From Snell's law we can also deduce that p_x and p_y are constant in such a medium. Hence, θ_x and θ_z only depend on the depth coordinate and remain constant with time. This is true irrespective of the actual shape of the plane wavefront and therefore of the actual velocity model present. Hence, simply put, plane waves in laterally homogeneous media are not subject to geometric spreading because the shape of the plane waves is laterally invariant and does not change over time, thus retaining a constant energy density or at least distribution. Furthermore, no assumptions have been made about the type and mode of the wavefront. Hence, a proper τ-p transform simultaneously removes the geometric spreading of all types and modes of waves (i.e., primary or multiple and pure-mode or converted waves) in laterally homogeneous media without prior knowledge of the actual underlying velocity model.

Some extra remarks need to be made. The term plane waves is misleading in that these waves are only planar in homogeneous media. The term quasi-plane would be more appropriate but is omitted for brevity. Likewise, the quasi-spherical instead of spherical t-x waves would be more justified.

The receivers can be located on any plane $z = z_r$, that is, they are not confined to be on the earth's surface and can lie, for instance, on the ocean bottom. However, the plane of receivers needs to be horizontal (or more generally interface parallel). This indicates, for instance, that the geometric spreading of data recorded in a VSP experiment with the receivers in the borehole cannot be corrected in a straightforward manner using the methodology described here.

REFERENCES

Alkhalifah, T., 1997, Velocity analysis using nonhyperbolic moveout in transversely isotropic media: Geophysics, **62**, 1839–1854.

Alkhalifah, T., and Tsvankin, I., 1995, Velocity analysis for transversely isotropic media: Geophysics, **60**, 1550–1566.

Brysk, H., and McCowan, D. W., 1986, A slant-stack procedure for point-source data: Geophysics, **51**, 1370–1386.

Chapman, C. H., 1981, Generalized Radon transforms and slant stacks: Geophysical Journal of the Royal Astronomical Society, **66**, 445–453.

Chapman, C. H., and Orcutt, J. A., 1985, The computation of body wave synthetic seismograms in laterally homogeneous media: Reviews of Geophysics, **23**, 105–163.

Dunkin, J. W., and Levin, F. K., 1973, Effect of normal moveout on a seismic pulse: Geophysics, **38**, 635–642.

Dunne, J., and Beresford, G., 1998, Improving seismic data quality in the Gippsland Basin (Australia): Geophysics, **63**, 1496–1506.

Fryer, G. J., and Frazer, L. N., 1984, Seismic waves in stratified anisotropic media: Geophysical Journal of the Royal Astronomical Society, **78**, 691–710.

——— 1987, Seismic waves in stratified anisotropic media—II. Elastodynamic eigensolutions for some anisotropic systems: Geophysical Journal of the Royal Astronomical Society, **91**, 73–101.

Fuchs, K., and Müller, G., 1971, Computation of synthetic seismograms with the reflectivity method and comparison with observations: Geophysical Journal of the Royal Astronomical Society, **23**, 417–433.

Gutenberg, B., 1936, The amplitudes of waves to be expected in seismic prospecting: Geophysics, **1**, 252–256.

Kendall, R. R., and Pullishy, J., 2002, A proposed workflow for converted-wave event registration—The step between processing and interpretation: 64th Annual Meeting, European Association of Geoscientists and Engineers, Extended Abstracts, P004.

Moon, W., Carswell, A., Tang, R., and Dilliston, C., 1986, Radon transform wave-field separation for vertical seismic profiling data: Geophysics, **51**, 940–947.

Newman, P., 1973, Divergence effects in a layered earth: Geophysics, **38**, 481–488.

O'Doherty, R. F., and Anstey, N. A., 1971, Reflections on amplitudes: Geophysical Prospecting, **19**, 430–458.

Phinney, R. A., Roy Chowdhury, K., and Frazer, L. N., 1981, Transformation and analysis of record sections: Journal of Geophysical Research, **86**, 359–377.

Schultz, P. S., 1982, A method for direct estimation of interval velocities: Geophysics, **47**, 1657–1671.

Stoffa, P. L., Diebold, J. B., and Buhl, P., 1981, Inversion of seismic data in the τ-p domain: Geophysical Research Letters, **8**, 869–872.

——— 1982, Velocity analysis of wide aperture seismic data: Geophysical Prospecting, **30**, 25–57.

Taner, M. T., and Koehler, F., 1969, Velocity spectra-digital computer derivation and applications of velocity functions: Geophysics, **34**, 859–881.

Thomsen, L., 1986, Weak elastic anisotropy: Geophysics, **51**, 1954–1966.

Treitel, S., Gutowski, P. R., and Wagner, D. E., 1982, Plane-wave decomposition of seismograms: Geophysics, **47**, 1375–1401.

Tsvankin, I., and Thomsen, L., 1994, Nonhyperbolic reflection moveout in anisotropic media: Geophysics, **59**, 1290–1304.

Ursin, B., 1990, Offset-dependent geometric spreading in a layered medium: Geophysics, **55**, 492–496.

Van der Baan, M., and Kendall, J.-M., 2002, Estimating anisotropy parameters and traveltimes in the τ-p domain: Geophysics, **67**, 1076–1086.

——— 2003, Traveltime and conversion-point computations and parameter estimation in layered, anisotropic media by τ-p transform: Geophysics, **68**, 210–224.

Wang, D. Y., and McCowan, D. W., 1989, Spherical divergence correction for seismic reflection data using slant stacks: Geophysics, **54**, 563–569.

Wang, Y., and Houseman, G. A., 1997, Point-source τ-p transform: A review and comparison of computational methods: Geophysics, **62**, 325–334.

Wapenaar, C. P. A., Verschuur, D. J., and Herrmann, P., 1992, Amplitude preprocessing of single and multicomponent seismic data: Geophysics, **57**, 1178–1188.

Wookey, J., Van der Baan, M., Smit, D., and Kendall, J.-M., 2002, Tau-p domain VTI parameter inversions using limited-offset data: 64th Meeting, European Association of Geoscientists and Engineers, Extended Abstracts, F041.

Yilmaz, O., 2001, Seismic data analysis—Processing, inversion, and interpretation of seismic data, 2nd ed.: Society of Exploration Geophysicists.

Zhou, H., and McMechan, G. A., 2000, Analytic study of geometric spreading of *P*-waves in a layered transversely isotropic medium with a vertical symmetry axis: Geophysics, **65**, 1305–1315.